Biochemical and Biophysical Research Communications 435 (2013) 255–259

Contents lists available at SciVerse ScienceDirect

Biochemical and Biophysical Research Communications

journal homepage: www.elsevier.com/locate/ybbrc

Crystal structure of *Mycobacterium tuberculosis* Rv2606c: A pyridoxal biosynthesis lyase

Sangwoo Kim [a,b], Kyung-Jin Kim [a,*]

[a] School of Life Science and Biotechnology, Kyungpook National University, Republic of Korea
[b] School of Nono-Bioscience and Chemical Engineering, Ulsan National Institute of Science and Technology (UNIST), Ulsan, Republic of Korea

ARTICLE INFO

Article history:
Received 18 April 2013
Available online 30 April 2013

Keywords:
Tuberculosis
Pyridoxal biosynthesis lyase
PdxS
Crystal structure

ABSTRACT

Tuberculosis is a lethal infectious disease caused by *Mycobacterium tuberculosis*. We determined the crystal structure of Rv2606c, a potential pyridoxal biosynthesis lyase (PdxS), from *M. tuberculosis* H37Rv at 1.8 Å resolution. The overall structure of the protein, composed of a $(\beta/\alpha)_8$-barrel and two small 3_{10}-helices, was quite similar to those of other PdxS proteins. A glycerol molecule was observed to be bound at the active site of the Rv2606c structure through interactions with the conserved residues of Asp29 and Lys86, providing information regarding the potential active site and the substrate-binding environment of the protein. The interface for Rv2606c dodecamerization, which is primarily mediated by salt bridges and hydrophobic interactions, was quite different from those of other PdxS proteins. Furthermore, we observed that the Rv2606c and Rv2604c form a stable complex, suggesting that these proteins might function as PdxS and PdxT in *M. tuberculosis*.

1. Introduction

Tuberculosis is an infectious bacterial disease caused by *Mycobacterium tuberculosis*, which most commonly affects the lungs [1]. In 2011, there were an estimated 8.7 million new cases of tuberculosis, with 1.4 million fatalities. While the number of cases of multidrug-resistant tuberculosis reported in the 27 high multidrug-resistant tuberculosis is increasing and reached almost 60,000 worldwide in 2011, the number constitutes only 19% of the reported tuberculosis patients estimated to have multidrug-resistant tuberculosis [2].

Multidrug-resistant and extensively drug-resistant tuberculosis is a major public health problem that threatens progress made in tuberculosis care and control worldwide [3,4]. Many studies have been carried out to better understand the multidrug-resistance mechanisms in tuberculosis [5–7]. Understanding the molecular mechanisms underlying drug resistance in tuberculosis is essential for the development of new drugs.

The biologically active form of vitamin B6 (pyridoxine or pyridoxal), referred to as pyridoxal 5′-phosphate (PLP), serves a cofactor in decarboxylation, deamination and transamination reactions [8–10]. The class I glutamine amidotransferase pathway is composed of pyridoxal biosynthesis lyase (PdxS, Pdx1) and glutamine amidotransferase subunits (PdxT, Pdx2) [11,12]. PLP is synthesized by PdxS using the NH_3 generated during the conversion of glutamine into glutamate by PdxT. There are independent pathways to generate PLP, which are known as deoxyxylulose 5-phosphate (DXP)-dependent pathways. While the DXP-dependent pathway, which was extensively studied in *Escherichia coli*, is limited to a small number of bacteria, the DXP-independent route is widespread among archaea, plants, fungi and most bacteria [13–16]. This pathway involves the interplay between two proteins, PdxS and PdxT, which jointly display glutamine amidotransferase activity.

The *M. tuberculosis* genome encodes homologs of proteins involved in the DXP-independent PLP biosynthetic pathway, PdxS (Rv2606c) and PdxT (Rv2604c). It has been demonstrated that *M. tuberculosis* synthesizes PLP via the DXP-independent pathway using PLP synthase, and that the disruption of the PdxS gene generates a vitamin B6 auxotrophic *M. tuberculosis* mutant. Organisms possess genes that encode PLP synthase to salvage PLP after it participates as a cofactor in enzymatic reactions. It is unclear whether *M. tuberculosis* can acquire PLP from the host. Recently, vitamin B6 biosynthesis has been known to be essential for the survival and virulence of *M. tuberculosis* in the mouse model [17]. Vitamin B6 biosynthesis may be an effective target pathway for the development of new tuberculosis agents.

In an effort to elucidate the molecular mechanism of vitamin B6 synthesis in *M. tuberculosis*, we report the crystal structure of Rv2606c, a potential PdxS protein of the strain. We also reveal that the Rv2606c protein forms a complex with Rv2604c, a potential PdxT protein.

* Corresponding author. Address: School of Life Science and Biotechnology, Kyungpook National University, Daegu 702-701, Republic of Korea. Fax: +82 53 955 5522.
E-mail address: kkim@knu.ac.kr (K.-J. Kim).

0006-291X/$ - see front matter © 2013 Elsevier Inc. All rights reserved.
http://dx.doi.org/10.1016/j.bbrc.2013.04.068

2. Materials and methods

2.1. Cloning, expression, and purification

Cloning, expression, purification, and crystallization of Rv2606c will be described elsewhere (Kim et al., in preparation). Briefly, The Rv2606c gene was amplified from the chromosomal DNA of *M. tuberculosis* H37Rv strain by a polymerase chain reaction (PCR). The PCR product was then subcloned into $pP_{RO}EX$ HTa (Invitrogen) with 6xHis at the N-terminus and a recombinant TEV protease (rTEV) cleavage site. The resulting expression vector $pP_{RO}EX$ HTa:*Rv2606c* was transformed into *E. coli* B834 strain and the cells were grown in an LB medium containing ampicillin at 310 K. After induction with 1.0 mM IPTG for a further 20 h at 295 K, the culture was harvested by centrifugation at 5000*g* at 277 K. The cell pellet was resuspended in ice-cold buffer A (40 mM Tris-HCl, pH 8.0, 5 mM of β-mercaptoethanol) and disrupted by ultrasonication. The cell debris was removed by centrifugation at 11,000*g* for 1 h, and lysate was bound to Ni-NTA agarose (QIAGEN). After washing with buffer A containing 20 mM imidazole, the bound proteins were eluted with 300 mM imidazole in buffer A. The 6xHis-tag was released from the Rv2606c by incubating with rTEV protease (GIBCO). A trace amount of contamination was removed by applying HiTrap Q HP (GE Healthcare) ion exchange and HiLoad 26/60 Superdex 200 prep grade (GE Healthcare) size exclusion chromatography. The purified protein showed ~95% purity on SDS-PAGE, was concentrated to 45 mg/ml in 40 mM Tris-HCl, pH 8.0, 1 mM dithiothreitol.

2.2. Crystallization and data collection

Crystallization of the purified protein was initially performed with crystal screening kits (Hampton Research and Emerald Biostructures) using the hanging-drop vapor-diffusion technique at 293 K. Each experiment consisted of mixing 1.5 μl protein solution (22 mg/ml in 20 mM Tris–HCl pH 8.0 and 5 mM β-mercaptoethanol) with 1.5 μl reservoir solution and then equilibrating it against 0.5 ml of the reservoir solution. The Rv2606c crystals with dimensions of $0.2 \times 0.2 \times 0.4$ mm was obtained from the condition of 8% PEG 8000, 0.1 M 3-[Cyclohexylamino]-1-propanesulfonic acid, pH 10.5 and 0.2 M sodium chloride. The data were collected at 100 K at 7A beamline of the Pohang Accelerator Laboratory (PAL, Pohang, Korea) using a Quantum 270 CCD detector (ADSC, USA). The data were then indexed, integrated, and scaled using the HKL2000 suite [18]. Crystals belonged to space group *I*222, with unit cell parameters of $a = 110.75$ Å $b = 126.08$ Å $c = 180.82$ Å, $\alpha = \beta = \gamma = 90°$. Assuming three molecules of Rv2606 per asymmetric unit, the crystal volume per unit of protein mass was 3.79 $Å^3$/Da [19], which corresponds to a solvent content of approximately 67.55%.

2.3. Structure determination

The structure of Rv2606c was solved by molecular replacement using the *Thermotoga maritima* PdxS (pdb code 2ISS) with the side chains converted to Ala as a search model. The identity and similarity of the 2ISS sequence to Rv2606c are 63 and 77%, respectively. MOLREP [20] located three poly-Ala model molecules in the asymmetric unit. Further model building was performed manually using the program WinCoot [21] and the refinement was performed with REFMAC5 [22]. The refined model of Rv2606 was deposited in the Protein Data Bank (PDB code 4JDY).

2.4. Site-directed mutagenesis

In order to obtain the $Rv2604c^{H170N}$ mutant protein, Site-directed mutagenesis experiment was performed using the primers 5′-TTGCCACCGCGTTTAATCCGGAGATGACCGG-3′ and 5′-CCGGTCA TCTCCGGATTAAACGCGGTGGCAA-3′. All oligonucleotides were purchased from BIONEER (Daejeon, Korea) in a salt-free grade.

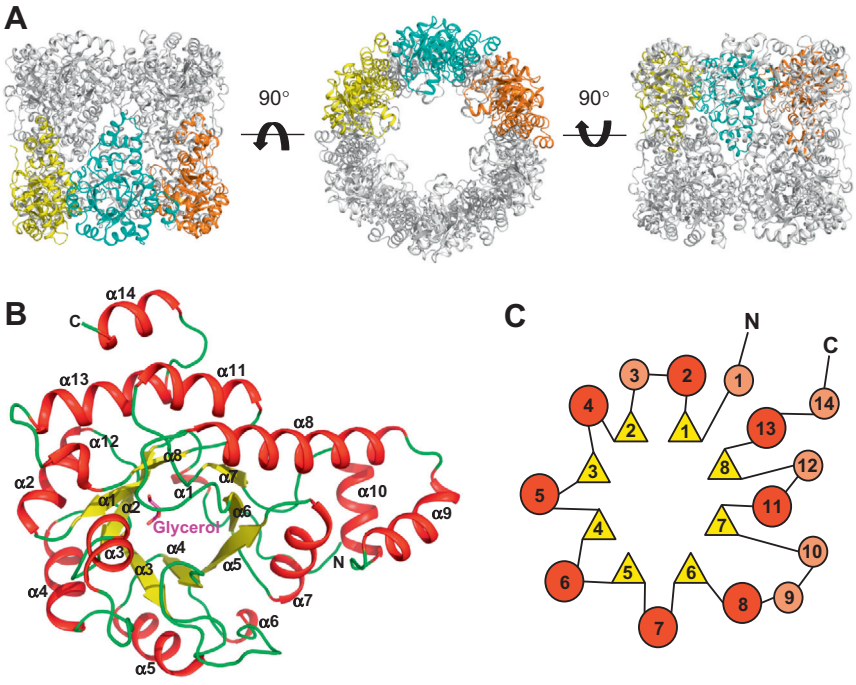

Fig. 1. Overall structure of Rv2606c. (A) A dodecameric structure of Rv2606c. The dodecameric structure of Rv2606c is presented as a cartoon diagram. The three molecules found in an asymmetric unit of *I222* crystal packing is distinguished with yellow, cyan and orange colors, and other molecules are shown with gray color. (B) A monomer structure of Rv2606c. The monomer structure of Rv2606c is presented as a cartoon diagram. Secondary structures of α-helices and β-sheets are colored by red and yellow colors, respectively, and appropriately labeled. (D) A schematic diagram of Rv2606c monomer. Secondary structures of α-helices and β-sheets are presented as circles and triangles, respectively. The α-helices involved in the formation of the $(\beta/\alpha)_8$-barrel are shown with red color, and other α-helices are with orange color. (For interpretation of the references to colour in this figure legend, the reader is referred to the web version of this article.)

3. Results and discussion

3.1. Overall structure

In order to address the structural basis for the catalytic mechanism of pyridoxal biosynthesis lyase of *M. tuberculosis*, we determined the 1.8 Å crystal structure of Rv2606c, a protein assigned as a potential pyridoxal biosynthesis lyase (PdxS). The asymmetric unit contains 3 Rv2606c molecules, and the dodecameric structure of the protein could easily be generated by applying crystallographic *I*222 symmetry (Fig. 1A). The data collection and refinement statistics are summarized in Table 1. The overall structure of Rv2606 is very similar to the structures of PLP synthases from *Thermotoga maritima* and *Bacillus subtilis* [23,24]. Their overall structures superpose with an RMSD of <1.0 Å (0.9 and 0.8 Å for *T. maritima* and *B. subtilis*, respectively). The monomer structure of Rv2606c has a $(\beta/\alpha)_8$-barrel fold, composed of an 8-stranded β-sheet (β*1*–β8), 12 α-helices (α1–α12) and 2 small 3_{10}-helices (η1–η2) (Fig. 1B and C). Furthermore, the overall structures of three molecules have the same root mean square deviation (RMSD) for the Cα: 0.139 (A and B), 0.140 (A and C), and 0.114 Å (B and C).

Table 1
Data collection and refinement statistics.

	Rv2606c
Data collection	
Space group	*I*222
Cell dimensions	
a, *b*, *c* (Å)	110.75, 126.08, 180.82
α, β, γ (°)	90.00, 90.00, 90.00
Resolution (Å)	50.00 – 1.80 (1.86 – 1.80)*
R_{sym} or R_{merge}	7.2 (32.8)
$I/\sigma I$	20.19 (2.38)
Completeness (%)	99.0 (97.0)
Redundancy	5.3 (3.8)
Refinement	
Resolution (Å)	50.00 – 1.80
No. reflections	109504
R_{work}/R_{free}	18.4/21.1
No. atoms	6304
Protein	5841
Ligand	18
Water	463
B-factors	23.23
Protein	23.61
Ligand	38.52
Water	27.01
R.m.s. deviations	
Bond lengths (Å)	0.030
Bond angles (°)	2.202

* Number of xtals for each structure should be noted in footnote. *Values in parentheses are for highest-resolution shell.

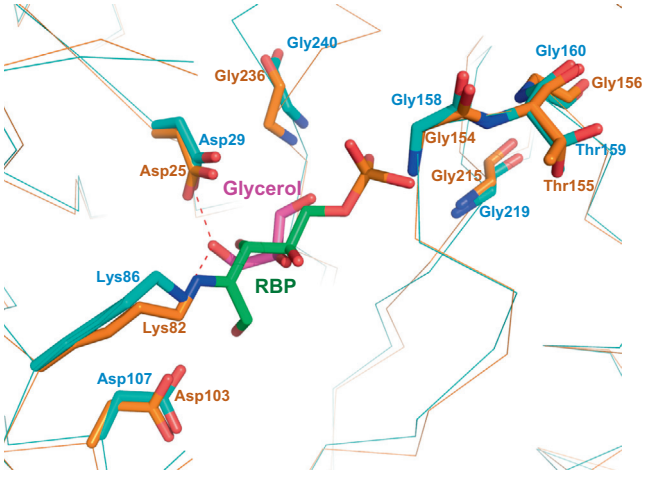

Fig. 2. The active site of Rv2606c. The crystal structures of Rv2606c and PdxS from *T. maritima* are superposed, and presented as ribbon diagrams with cyan and orange colors, respectively. The residues involved in the enzyme catalysis, the substrate binding and the Gly-Thr-Gly motif of PdxS from *T. maritima* are shown as stick models with orange color, and those of Rv2606c are with cyan color. The RBP substrate bound at the PdxS from *T. maritima* and the glycerol molecule bound at Rv2606c are shown as stick models with green and magenta colors, respectively. (For interpretation of the references to colour in this figure legend, the reader is referred to the web version of this article.)

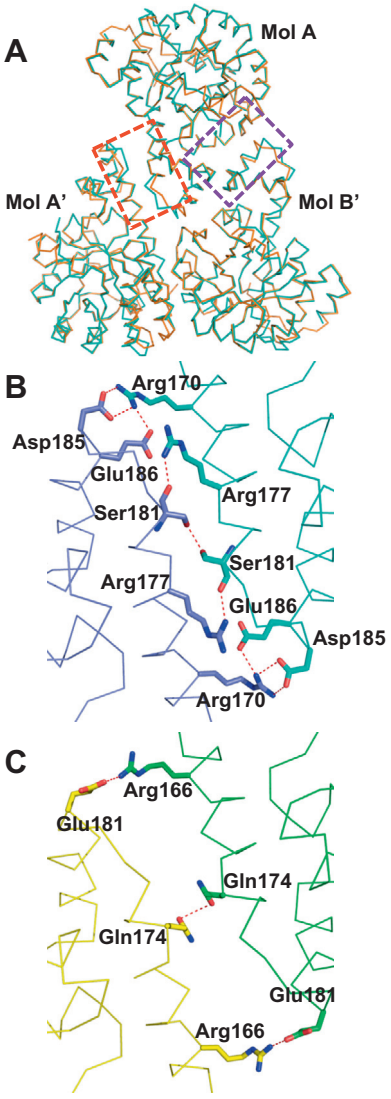

Fig. 3. Interfaces for the formation of dodecameric structure. (A) The crystal structures of Rv2606c and PdxS from *T. maritima* are superposed, and presented as ribbon diagrams with cyan and orange colors, respectively. Mol A represents one molecule from one hexamer, and Mol A' and Mol B' do two adjacent molecules from another hexamer. The interface between Mol A and Mol A′, and the between Mol A and Mol B' are shown as dotted-rectangles with red and pepper colors, respectively. (B) The dodecamerization interface of Rv2606c. The interface between Mol A and Mol A′ for the dodecamerization of Rv2606c is presented. Mol A and Mol A′ are shown as ribbon diagrams with cyan and marine colors, respectively. Residues involved in the hydrogen bonds are shown as stick models, and the hydrogen bonds are dotted-lines. (C) The dodecamerization interface of PdxS from *T. maritima*. Mol A and Mol A′ are shown as ribbon diagrams with green and yellow colors, respectively. Hydrogen bonds and the residues involved in the hydrogen bonds are similarly presented as shown in (B). (For interpretation of the references to colour in this figure legend, the reader is referred to the web version of this article.)

3.2. Active site structure

Structural comparison of our structure with that of PdxS from *T. maritima* leads us to identify the active site of Rv2606c [24]. In the active site of PdxS from *T. maritima*, the ribulose moiety of the ribulose 5-phosphate (RBP) substrate was bound through hydrogen bonds to the Asp25, Lys82 and Asp103 residues, and the phosphate moiety of RBP was bound to the main chain nitrogen atoms of Gly154, Gly215 and Gly236 (Fig. 2). In the Rv2606c structure, a glycerol molecule was observed bound at the position of the ribulose moiety of RBP. The bound glycerol molecule was stabilized through hydrogen bonds the Asp29 and Lys86 residues, which correspond to the Asp25 and Lys82 residues in *T. maritima* PdxS. The Asp103 residue of Rv2606c was also located at the position similar to that of the Asp103 residue of *T. maritima* PdxS. Moreover, in the Rv2606c structure, three glycines (at positions 158, 219 and 240) were observed at positions similar to those of Gly154, Gly215, and Gly236 from *T. maritima* PdxS, indicating that the phosphate moiety of RBP might be similarly recognized in the active site of Rv2606c (Fig. 2). It is reported that, in PdxS from *T. maritima*, the β6–α8 loop containing the Gly154-Thr155-Gly156 motif undergoes a structural change upon substrate binding [25]. In our structure, the Gly158-Thr159-Gly160 motif was conserved as well. Based on these observations, we suggest that the Rv2606c protein might recognize an RBP substrate in a mode similar to that of *T. maritima* PdxS.

3.3. Oligomerization

In the crystal structures of PdxS proteins from *T. maritima* and *B. subtilis*, two hexameric rings assemble to form a dodecameric structure of the protein [23,24]. The Rv2606c protein also forms a dodecamer, which is consistent with the results of size exclusion chromatography (data not shown). The interfaces forming a hexameric structure in Rv2606c are observed to be quite similar to those of the PdxS protein from *T. maritima* and *B. subtilis*. The hexamer appears to be stabilized through salt bridges (Glu73, Arg88, Asp116, Arg170, Asp225, and Arg274), hydrogen bonds (Arg65, Gln96, Ala115, Gly160, Thr166, and Gln231), and hydrophobic interactions (Phe92, Val93, Ala224, Met228 and Leu232), and the residues involved in hexamerization are highly conserved with those of PdxS from *T. maritima* and *B. subtilis*. To form a dodecamer, molecule A of one hexamer contacts with two molecules (A′ and B′) of another hexamer (Fig. 3A). The interface between molecules A and B′ is primarily stabilized through hydrophobic interactions mediated by the residues Ala118, Phe188, Val189, and Tyr198, which is quite similar to that of the PdxS proteins from *T. maritima* and *B. subtilis*. However, the interface between molecule A and A′ is quite unique in the Rv2606c structure. Compared with PdxS from *T. maritima*, where only a few hydrogen bonds are involved in the stabilization of the interface between molecule A and A′, that of Rv2606c appears to be stabilized by more hydrogen bonds be-

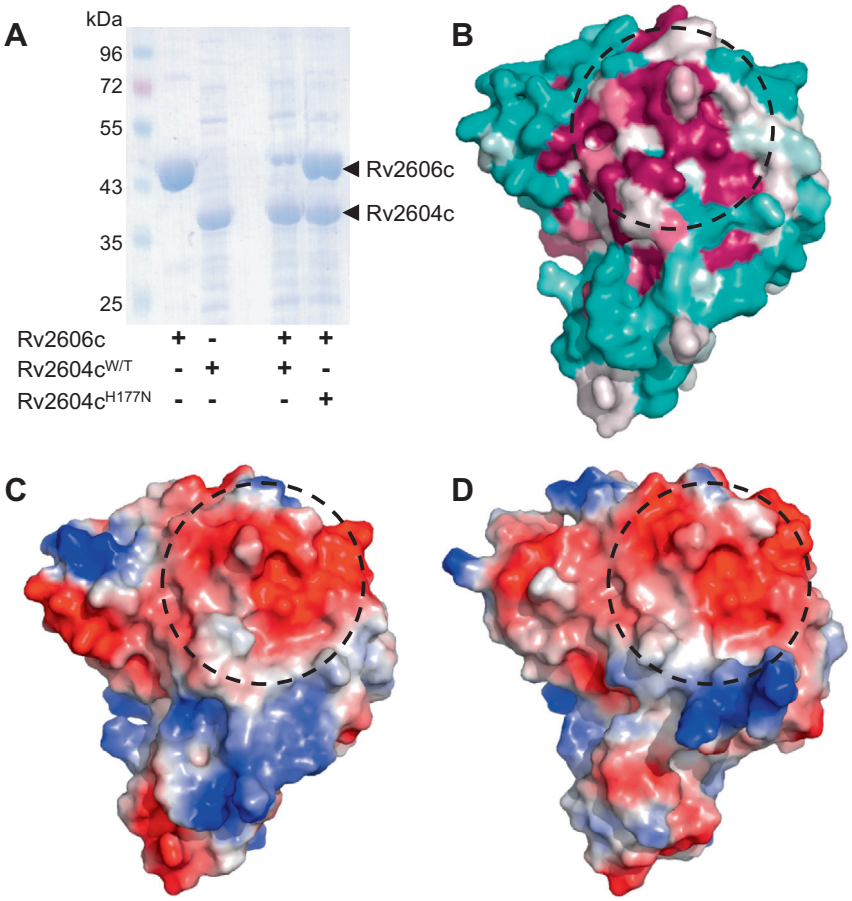

Fig. 4. Complex formation of Rv2606c/Rv2604c. (A) An SDS-PAGE of the complex formation between Rv2606c and Rv2604c. The Rv2606c$^{W/T}$ protein and Rv2606c^{H177N} mutant protein are purified as native forms, and Rv2604c is as 6x-histagged protein at the C-terminal end. (B) Surface presentation of Rv2606c. The amino acid residue conservation level of Rv2606c is presented with surface model. Pepper, light pepper, gray and cyan colors represent from the highest and lowest level of amino acid conservation. The Rv2604c binding region of Rv2606c is shown with black dotted-line. (C and D) Surface electrostatic potential presentation of Rv2606c (C) and PdxS from *T. maritima* (D). The monomer structures of Rv2606c and PdxS from *T. maritima* are shown as surface electrostatic potential models. The Rv2604c and PdxS binding regions of Rv2606c and PdxS from *T. maritima*, respectively, are shown with black dotted-lines. (For interpretation of the references to colour in this figure legend, the reader is referred to the web version of this article.)

tween unique residues such as Arg170, Arg177, Ser181, Asp185, and Glu186 (Fig. 3B and C).

3.4. Complex formation with Rv2604c

It has been reported that PdxS transiently interacts with PdxT (glutamine amidotransferase), and that these two proteins perform their reactions consecutively [23,26]. PdxS synthesizes PLP from ribulose-5-phosphate by the addition of the NH_3 ion, which is produced from the conversion of glutamine to glutamate by PdxT. It is known that 12 PdxT subunits are attached to outside two hexameric rings formed by the 12 PdxS subunits like the cogs of a gear wheel, and that a mutation on the His170 catalytic residue of PdxT leads the protein to form a permanent complex with PdxS in *B. subtilis*[23]. We found that the gene coding for Rv2604c is located in the same operon as that of Rv2606c in the *M. tuberculosis* chromosome, and the protein shows high amino acid identity with the PdxT proteins of other microorganisms. In order to obtain the Rv2606c/Rv2604c complex, we generated an Rv2604c mutant by replacing the His177 residue, corresponding residue to His170 of *B. subtilis*, with aspargine, and incubated the $Rv2604c^{H177N}$ protein with the recombinant Rv2606c protein in the presence of glutamine. The $Rv2604c^{H177N}$ mutant protein forms a stable complex with Rv2606c, while the wild-type Rv2604c does not (Fig. 4A). These results indicate that Rv2604c is a homolog of *M. tuberculosis* PdxT, and that Rv2604c and Rv2606c catalyze the production of PLP via the same mechanism as that of PdxS/PdxT of *T. maritima* and *B. subtilis*. Although we could not obtain a crystal of the $Rv2604c^{H177N}$/Rv2606c complex, the structural comparison of Rv2606c with the PdxS proteins of *T. maritima* and *B. subtilis* leads us to predict the binding mode between the Rv2606c and Rv2604c proteins.

The complex structure of PdxS/PdxT from *B. subtilis* shows that in the N-terminal region, the connecting loops between α1–β1 and α5–β4 of PdxS interact with PdxT through charge–charge interactions. Furthermore, structural and amino acid sequence comparison between PdxS from *B. subtilis* and Rv2606c reveal that the PdxT binding region of PdxS from *B. subtilis* is highly conserved in the putative Rv2604c-binding region of Rv2606c (Fig. 4B). Electrostatic surface potential analysis of Rv2606c shows that, as observed in the PdxT binding region of PdxS from *B. subtilis*, the connecting loops between α1–β1 and α5–β4, and the N-terminal region of Rv2606c form a highly charged patch comprised of highly charged residues, such as Arg16, Lys23, and Asp104 (Fig. 4C and D). Based on these observations, we suggest that complex formation between Rv2606c and Rv2604c might be mediated through electrostatic interactions. Taken together, we suggest that the Rv2606c and Rv2604c proteins function as PdxS and PdxT proteins in *M. tuberculosis*, and their reaction mechanism might be similar to those of the PdxS/PdxT proteins of *B. subtilis* and *T. maritima*.

Acknowledgments

This work was supported by the National Research Foundation of Korea (NRF) Grant funded by the Korean Government (MEST) (NRF-2009-C1AAA001-2009-0093483) and by the Advanced Biomass R&D Center (ABC) of Global Frontier Project funded by the MEST (ABC- 2012-053895), and also funded by a part of the project titled "Gyeongbuk Sea Grant Program" funded by the MLTM, Korea.

References

[1] S.S.C. Dye, P. Dolin, V. Pathania, M.C. Raviglione, Consensus statement. Global burden of tuberculosis: estimated incidence, prevalence, and mortality by country. WHO Global Surveillance and Monitoring Project., J. Am. Med. Assoc. 18 (1999) 677–686.
[2] R. Coker, Review: multidrug-resistant tuberculosis: public health challenges, Tropical Med. Int. Health 9 (2004) 25–40.
[3] S.S. Shin, C.D. Mitnick, K.J. Seung, M.L. Rich, S.S. Atwood, J.J. Furin, G.M. Fitzmaurice, F.A. Alcantara Viru, S.C. Appleton, J.N. Bayona, C.A. Bonilla, K. Chalco, S. Choi, M.F. Franke, H.S. Fraser, D. Guerra, R.M. Hurtado, D. Jazayeri, K. Joseph, K. Llaro, L. Mestanza, J.S. Mukherjee, M. Muñoz, E. Palacios, E. Sanchez, A. Sloutsky, M.C. Becerra, Comprehensive treatment of extensively drug-resistant tuberculosis, N. Engl. J. Med. 359 (2008) 563–574.
[4] G. Friedland, S. Shenoi, Extensively drug-resistant tuberculosis: a new face to an old pathogen, Annu. Rev. Med. 60 (2009) 307–320.
[5] A. Sandgren, M. Strong, P. Muthukrishnan, B.K. Weiner, G.M. Church, M.B. Murray, Tuberculosis drug resistance mutation database, PLoS Med. 6 (2009) 132–136.
[6] D.M. Sp Klemens, M.H. Cynamon, Therapy of multidrug-resistant tuberculosis: lessons from studies with mice, Antimicrob. Agents Chemother. 37 (1993) 2344–2347.
[7] S. Do, J.R. Bolla, F. Long, L. Dai, C.C. Su, H.T. Lei, X. Chen, J.E. Gerkey, D.C. Murphy, K.R. Rajashankar, Q. Zhang, E.W. Yu, Structural and functional analysis of the transcriptional regulator Rv3066 of Mycobacterium tuberculosis, Nucleic Acids Res. 40 (2012) 9340–9355.
[8] H. Hayashi, Pyridoxal enzymes: mechanistic diversity and uniformity, J. Biochem. 118 (1995) 463–473.
[9] R. John, Pyridoxal phosphate-dependent enzymes, Biochim. Biophys. Acta 1248 (1995) 81–96.
[10] K.J. Ac Eliot, Pyridoxal phosphate enzymes: mechanistic, structural, and evolutionary considerations, Annu. Rev. Biochem. 73 (2004) 383–415.
[11] Y. Xiang, K.E. Burns, C.L. Kinsland, F.W. McLafferty, T.P. Begley, Reconstitution and biochemical characterization of a new pyridoxal-5′-phosphate biosynthetic pathway, J. Am. Chem. Soc. 23 (2005) 3682–3683.
[12] F.T.M. Gengenbacher, T. Raschle, K. Flicker, I. Sinning, S. Müller, P. Macheroux, I. Tews, B. Kappes, Vitamin B6 biosynthesis by the malaria parasite Plasmodium falciparum: biochemical and structural insights, J. Biol. Chem. 10 (2006) 3633–3641.
[13] E.K. My Galperin, Sequence analysis of an exceptionally conserved operon suggests enzymes for a new link between histidine and purine biosynthesis, Mol. Microbiol. 24 (1997) 443–445.
[14] G. Mittenhuber, Phylogenetic analyses and comparative genomics of vitamin B6 (pyridoxine) and pyridoxal phosphate biosynthesis pathways, J. Mol. Microbiol. Biotechnol. 3 (2001) 1–20.
[15] P. Js Seack, V. Gamulin, H.C. Schroder, P. Beutelmann, I.M. Muller, W.E. Muller, Identification of highly conserved genes: SNZ and SNO in the marine sponge Suberites domuncula: their gene structure and promoter activity in mammalian cells, Biochim. Biophys. Acta 1520 (2001) 21–34.
[16] V. Vanniasingham, S. Sivasubramaniam, C.T. Tan, N.H. Chua, Characterisation of HEVER, a novel stress-induced gene from Hevea brasiliensis, Plant Mol. Biol. 29 (1995) 173–178.
[17] M.U.T. Dick, B. Kappes, M. Gengenbacher, Vitamin B6 biosynthesis is essential for survival and virulence of Mycobacterium tuberculosis, Mol. Microbiol. 78 (2010) 980–988.
[18] W. Minor, Z. Otwinowski, Processing of X-ray diffraction data collected in oscillation mode, Methods Enzymol. 276 (1997) 307–326.
[19] B. Matthews, Solvent content of protein crystals, J. Mol. Biol. 28 (1968) 491–497.
[20] Collaborative Computational Project, The CCP4 suite: programs for protein crystallography, Acta Crystallogr. D Biol. Crystallogr. 1 (1994) 760–763.
[21] K. Cowtan, P. Emsley, Coot: model-building tools for molecular graphics, Acta Crystallogr. D Biol. Crystallogr. 60 (2004) 2126–2132.
[22] V.A. Gn Murshudov, E.J. Dodson, Refinement of macromolecular structures by the maximum-likelihood method, Acta Crystallogr. D Biol. Crystallogr. 1 (1997) 240–255.
[23] T. Raschle, M. Strohmeier, J. Mazurkiewicz, K. Rippe, I. Sinning, T.B. Fitzpatrick, I. Tews, Structure of a bacterial pyridoxal 5′-phosphate synthase complex, Proc. Natl. Acad. Sci. USA 19 (2006) 19284–19289.
[24] Z.Y.F. Zein, Y.N. Kang, K. Burns, T.P. Begley, S.E. Ealick, Structural insights into the mechanism of the PLP synthase holoenzyme from thermotoga maritima, Biochemistry 12 (2006) 14609–14620.
[25] B.T. Rk Wierenga, M.E. Noble, Crystallographic binding studies with triosephosphate isomerases: conformational changes induced by substrate and substrate-analogues, FEBS Lett. 307 (1992) 34–39.
[26] A.N.T. Raschle, T.B. Fitzpatrick, On the two components of pyridoxal 5′-phosphate synthase from Bacillus subtilis, J. Biol. Chem. 16 (2005) 32291–32300.